



ELSEVIER

Journal of Electron Spectroscopy and Related Phenomena 127 (2002) 17–28

JOURNAL OF
ELECTRON SPECTROSCOPY
and Related Phenomena

www.elsevier.com/locate/elspec

One, two and three-body channels of the core–valence–valence Auger photoelectron coincidence spectra of early transition metals

Andrea Marini*, Michele Cini

Dipartimento di Fisica, Istituto Nazionale di Fisica della Materia, Universita' di Roma Tor Vergata, Via della Ricerca Scientifica, 1-00133 Rome, Italy

Abstract

We propose a simple model of core–valence–valence Auger and APECS intensities from open-band solids to account for the alleged negative- U behavior of the spectra of early transition metals. In these systems the maximum of the line shape is shifted by the interaction to lower binding energy, which is the contrary of what happens in closed band materials where the two-hole Green's function $G_{\omega}^{(2)}$ allows to understand the phenomenology of the spectra in terms of the U/W ratio of the on-site repulsion U to the band width W . Actually, for open-band solids, only part of the intensity comes from the decay of unscreened core-holes and is obtained by the two-body Green's function $G_{\omega}^{(2)}$, as in the case of filled bands. The rest of the intensity which arises from screened core-holes here is derived using a variational description of the relaxed ground state; this involves the two-holes-one-electron propagator G_{ω} , that also contains one-hole contributions. We propose a practical scheme to calculate the three-body Green function by a summation of the perturbation series to all orders. We achieve that by formally rewriting the problem in terms of a fictitious three-body interaction. Our method grants non-negative densities of states, explains the apparent negative- U behavior and interpolates well between weak and strong coupling, as we demonstrate by test model calculations.

© 2002 Elsevier Science B.V. All rights reserved.

Keywords: Electron impact; Auger emission; Photoemission and photoelectron spectra

PACS: 79.20.Fv; 79.60.-i

1. Introduction

The one-step model [1] of the core–valence–valence (CVV) Auger spectra coherently describes the ionization process and the Auger decay; the excitations due to the core level ionization do, in general, mix their amplitudes in the Auger decay. For solids with closed valence bands no electron–hole excitations are possible and the valence electrons remain

frozen during the ionization so that the spectra is well described [2] in terms of the two-holes Green's function $G_{\omega}^{(2)}$ by the Cini [3,4] and Sawatzky [5] (CS) model.

The CS model explains the phenomenology involving band-like, atomic-like and intermediate situations in terms of the U/W ratio of the on-site repulsion U to the band width W . For low U/W , the line shape is close to the self-convolution on the local one-hole density of states; with increasing U/W , the shape is distorted until, for a critical value of

*Corresponding author.

the ratio, two-hole resonances appear. Detailed studies of noble transition metals, like Au [6] and Ag [7] led to a very good agreement between theory and experiment, and also allowed the direct observation of off-site interaction effects [8]. In all these cases the diagrammatic expansion of $G_\omega^{(2)}$ is just a ladder of successive interactions between the two bare holes.

For almost completely filled bands, when the number of holes per quantum state $n_h \ll 1$, closed-band theory can be extrapolated [9]. The core-hole screening diagrams are $O(n_h)$ and one can assume again that, to a first approximation, the valence electrons remain frozen during the core ionization, and in the initial state of the Auger decay the valence configuration is the same as in the ground state. The CVV spectra are still essentially described in terms of the two-hole Green's function $G_\omega^{(2)}$, computed in the absence of the core hole. Using Galitzkii's low density approximation [10] (LDA) the dominant diagrams of the perturbation expansion of the $G_\omega^{(2)}$ are just the same ladder diagrams which provide the exact solution for $n_h \rightarrow 0$ [11,12]. This is the bare ladder approximation (BLA) that has been useful to interpret, e.g. the line shape of graphite [13]. The unexpected result was that the BLA is far better than the self-consistent ladder approximation.

The next turn came from experiments on early 3d transition metals, like Ti and Sc [14], that could not be interpreted by the above theory. The maximum of the line shape results shifted by the interaction to lower binding energy, which is the contrary of what happens in closed band materials. Qualitatively the CS model could work if one admitted that $U < 0$, and such an explanation has actually been proposed [15].

However, no justification of $U < 0$ exists; rather, $U > 0$ and the theory for almost empty bands is no simple extrapolation of the closed-band approach. pairing by positive U is actually possible (see e.g. M. Cini and A. Balzarotti, Phys. Rev. B. 56, 14711 (1997)) but this requires lobes sitting on different sites.

Sarma [16] first suggested that the Auger line shape of Ti looks like some linear combination of the one-electron density of states and its convolution. Using this hint, and the general framework of the one-step model, a simplified microscopic theory of

the apparent negative- U behavior was proposed by Cini and Drchal [17].

In this theory, the Auger line shape has two main contributions, that we call unrelaxed and relaxed, respectively. The unrelaxed contribution is obtained assuming that the Auger decay occurs while the conduction electrons are in their ground state $|\psi\rangle$ in the absence of the core hole. The density of states which shows up in this contribution is obtained by $G_\omega^{(2)}$, like in closed-band systems. However the screening electronic cloud that surrounds the core-hole can participate in the Auger decay; this contribution to the total current is described by the Auger decay with the ground state $|\phi\rangle$ in the presence of the core hole as initial state. We show that this last term is related to the Fourier transform of the $t > 0$ part of a three-body Green's function much harder to calculate than $G_\omega^{(2)}$. To sum the perturbation series of this complex many-body propagator we propose a simple approach in the spirit of the BLA [18].

Experimentally, one can single out the relaxed contribution to the total Auger current by properly fixing the photoelectron energy in an Auger photoelectron coincidence spectroscopy (APECS) experiment [19–22], where the Auger electron is detected in coincidence with the photoelectron responsible of the core hole creation.

2. From the one-step model to the two-body Green's functions

In the one-step model, the APECS current [1] is given by:

$$J(\epsilon_p, \epsilon_k) \sim \sum_j \frac{|\langle \Psi_0^N | \Phi_j^{N-1} \rangle|^2 \langle \Phi_j^{N-1} | A_k^\dagger (\omega_\gamma + E_0 - H(1) - \epsilon_p - \epsilon_k) A_k | \Phi_j^{N-1} \rangle}{(\omega_\gamma + E_0 + E_c - E_j - \epsilon_p)^2 + \Gamma^2} \quad (1)$$

with ϵ_p , ϵ_k are the photoelectron, Auger electron energies, E_c is the core level energy, ω_γ the incoming photon energy, Γ the Auger width of the core hole and A_k is the Auger operator. Since the algebra is complicated, we seek simplification by physical arguments. We write:

$$A_k = \sum_{\alpha\beta} M_{ck\alpha_1\beta_1} a_{\alpha_1} a_{\beta_1} \quad (2)$$

with $M_{ck\alpha_i\beta_i}$ Auger matrix elements; α_i, β_i are the *local* orbitals that belong to the Auger site that is, the site where the primary core-hole belongs; we will consider only the *local* scattering at the Auger site, since in this way we drastically simplify the algebra, and the line shape is little influenced by scattering at the other sites [23]. Many Auger line shape calculations in solids performed in this way have shown that this is a good approximation. Let $|\Psi_0^N\rangle$ be the ground state, with energy E_0^N , of the system with the core electron; the fully interacting valence electrons are described by the Hamiltonian:

$$H(n_c) = H(1) + (1 - n_c) \delta H \quad (3)$$

$n_c = 0, 1$ is the number of electrons in the core level. $\{|\Phi_j^{N-1}\rangle\}$ are the complete set of eigenstates of $H(0)$ (so in presence of the core hole), with energies $\{E_j^{N-1}\}$. N represents the total number of electrons. $H(n_c)$ contains the electron–electron interaction and the screening mechanism switched on by the ionization via the δH potential. then Eq. (1) describes the evolution of $|\Psi_0^N\rangle$ to each possible eigenstate $|\Phi_j^{N-1}\rangle$ in presence of the core-hole and the successive Auger decay. The summation on the excited state $|\Phi_j^{N-1}\rangle$ is the origin of the correlation between the photoelectron and the Auger energy measured in APECS experiments: tuning the photoelectron energy it's possible to select (within the Auger width Γ) the events corresponding to the decay of a few dominant intermediate states in the presence of the core hole [24].

The final two-hole density of states is complicated by the excitations present in the states $|\Phi_j^{N-1}\rangle$. These are due to the screening attractive interaction δH between the core hole and the valence electrons. Only for full bands systems there are no empty states to create hole–electron pairs necessary to screen the core hole; in this case Eq. (1) is greatly simplified because the valence electrons remain frozen during the ionization and so the summation over the states $\{|\Phi_j^{N-1}\rangle\}$ is well approximated by the ground state $|\Phi_0^{N-1}\rangle \approx |\Psi_0^N\rangle$, with the result:

$$\begin{aligned} & J(\epsilon_p, \epsilon_k) \\ & \sim J_{\text{XPS}}(\epsilon_p) \sum_{\alpha_1, \beta_1} \sum_{\alpha'_1, \beta'_1} M_{ck\alpha_1\beta_1}^* M_{ck\alpha_1\beta_1} D^{(2)}(\alpha_1\beta_1, \beta'_1\alpha'_1; \epsilon_p \\ & \quad + \epsilon_k - \omega_\gamma) \end{aligned} \quad (4)$$

where:

$$D^{(2)}(\alpha_1\beta_1, \beta'_1\alpha'_1; \omega) = -\frac{1}{\pi} \Im [\text{FT}(\theta(t) G^{(2)}(\alpha_1\beta_1, \beta'_1\alpha'_1; t))] \quad (5)$$

$$G^{(2)}(\alpha_1\beta_1, \beta'_1\alpha'_1; t) = (-i)^2 \langle \Psi_0^N | \text{T} \{ a_{\alpha_1}^\dagger(t) a_{\beta_1}^\dagger(t) a_{\beta'_1} a_{\alpha'_1} \} | \Psi_0^N \rangle \quad (6)$$

Here, FT stands for Fourier transform and operators are in the Heisenberg picture. As above we are using a special notation $\alpha_i, \beta_i \dots$ to indicate the set of quantum numbers of the *local* valence spin–orbitals belonging to the Auger site.

If we assume that the Coulomb valence–valence interaction between the orbitals of the Auger site is:

$$H_U = \sum_{\mu_1 < \nu_1, \rho_1 < \tau_1} U_{\mu_1\nu_1\rho_1\tau_1} a_{\mu_1}^\dagger a_{\nu_1}^\dagger a_{\tau_1} a_{\rho_1} \quad (7)$$

the two Auger holes dynamics contained in $H(1)$ is solved exactly in the CS model summing all orders of the perturbation series of the two-hole Green Function $G_\omega^{(2)}$. The diagrammatic method develops Eq. (6) in terms of local non-interacting time ordered one-body propagator $S_0(\alpha_i, \beta_i; t)$:

$$S_0(\alpha_i, \beta_i; t) = S_0^h(\alpha_i, \beta_i; t) - S_0^e(\beta_i, \alpha_i; -t) \quad (8)$$

where:

$$S_0^h(\alpha_i, \beta_i; t) = -i\theta(t) \langle a_{\alpha_i}^\dagger(t) a_{\beta_i} \rangle \quad (9)$$

$$S_0^e(\beta_i, \alpha_i; -t) = -i\theta(-t) \langle a_{\beta_i} a_{\alpha_i}^\dagger(t) \rangle \quad (10)$$

Here the average is taken over the non-interacting ground state $|\psi_0\rangle$ with energy E_0 . Introducing the non-interacting two-hole propagator:

$$g(\alpha_1\beta_1, \tau_1\rho_1; t - t_1) = \langle T \{ a_{\alpha_1}^\dagger(t) a_{\beta_1}^\dagger(t) a_{\tau_1}(t_1) a_{\rho_1}(t_1) \} \rangle \quad (11)$$

the final form of $G_i^{(2)}$ within CS theory is:

$$\begin{aligned} G^{(2)}(\alpha_1\beta_1, \beta'_1\alpha'_1; t) &= g(\alpha_1\beta_1, \beta'_1\alpha'_1; t) - i \sum_{\mu_1 < \nu_1, \rho_1 < \tau_1} U_{\mu_1\nu_1\rho_1\tau_1} \\ & \int_{-\infty}^{\infty} dt_1 g(\alpha_1\beta_1, \tau_1\rho_1; t - t_1) G^{(2)}(\mu_1\nu_1, \beta'_1\alpha'_1; t_1) \end{aligned} \quad (12)$$

Going to frequency space, this becomes a linear algebraic system. For almost completely filled bands,

when the number of holes per quantum state $n_h \ll 1$, closed-band theory can be extrapolated [9] leading to the same Eq. (12).

Eq. (12) works also for $n_h < 0.25$ and a range of U/W , however for open bands systems Eq. (12) is a partial sum of the perturbation series called bare ladder approximation (BLA) because it uses undressed single particle propagators. Cluster calculations [25] has shown that is a cancellation of self-energy and vertex corrections that permits the extension of the ladder expansion for $G_\omega^{(2)}$ to larger n_h .

The convolution form of Eq. (12) has further important consequences. Formally, it is a Dyson equation in which the U matrix is an instantaneous self-energy. Therefore, it grants the Herglotz property: for any interaction strength, $G^{(2)}$ generates a non-negative densities of states. The Herglotz property is a basic requirement for a sensible approximation, yet it is not easily obtained by diagrammatic approaches.

3. A variational approach to the negative- U problem

The above theory, neglecting the summation on the excited states $|\phi_j^{N-1}\rangle$, works well for full or nearly full bands but fails for early d transition metals. For these systems a rearrangement of the valence electrons after the creation of the core-hole must be included; in a simplified one-step approach to this problem [17], Eq. (1) is rewritten as:

$$J(\epsilon_p, \epsilon_k) \approx J_{\text{relaxed}}(\epsilon_p, \epsilon_k) + J_{\text{unrelaxed}}(\epsilon_p, \epsilon_k) \\ \propto \Gamma \left[\frac{D_{\phi\phi}(\epsilon_p + \epsilon_k - \omega_\gamma)}{(\omega_\gamma + E_c^{\text{rel}} - \epsilon_p)^2 + \Gamma^2} + \frac{D_{\psi\psi}(\epsilon_p + \epsilon_k - \omega_\gamma)}{(\omega_\gamma + E_c - \epsilon_p)^2 + (\Gamma + \delta)^2} \right] \quad (13)$$

with:

$$D_{\psi\psi}(\omega) = \langle \psi | A_k^\dagger \delta(\omega + H(1) - E) A_k | \psi \rangle \quad (14)$$

$$D_{\phi\phi}(\omega) = \langle \phi | A_k^\dagger \delta(\omega + H(1) - E) A_k | \phi \rangle \quad (15)$$

The physical idea is that the summation over the states $|\Phi_j^{N-1}\rangle$ in Eq. (1) is largely exhausted by summing over just two orthogonal states, namely, the ground state $|\psi\rangle$ of $H(1)$ with energy E and the relaxed initial state of the Auger transition, $|\phi\rangle$, that

is, the ground state of the valence electrons in the presence of the core-hole potential.

In this scheme, the Auger spectrum has two main contributions, *relaxed* and *unrelaxed*; the latter depends on $D_{\psi\psi}(\omega)$, which is analogous to that calculated for closed bands materials.

The relaxed contribution arises from creating the two Auger hole in the state $|\phi\rangle$ which is totally relaxed around the core-hole (that due to the screening cloud has a binding energy $E_c^{\text{rel}} \leq E_c$). Screening effects that permit the decay of $|\psi\rangle$ into $|\phi\rangle$ are described by the screening-width δ and it's interesting to note that for long-lived core-hole, when $\Gamma/\delta \ll 1$, the total current is dominated by the relaxed contribution $J_{\text{relaxed}}(\epsilon_p, \epsilon_k)$.

The electronic structure of the state $|\phi\rangle$ is calculated in Ref. [17] using a d -times degenerate Hamiltonian of Hubbard type:

$$H(0) = H_0 + H_{e-e} + H_{c-h} \quad (16)$$

where:

$$H_0 = \sum_{k\alpha} E(k) n_{k\alpha} \quad (17)$$

is the band term, H_{e-e} is the Hubbard interaction term, and:

$$H_{c-h} = -W \sum_{\alpha_1} n_{\alpha_1} \quad (18)$$

describes the coupling of the valence electrons to the core hole at the origin. Here $n_{k\alpha} = a_{k\alpha}^\dagger a_{k\alpha}$ are number operators in the Bloch representation.

The state $|\phi\rangle$ can be obtained from $|\psi\rangle$ by creating an infinite number of electron-hole pairs [26], and it is orthogonal to $|\psi\rangle$, $\langle \psi | \phi \rangle = 0$ (the so-called Anderson orthogonality catastrophe). On the other hand, the photoemission and Auger spectra can be calculated with high accuracy, if one includes only the one and two electron-hole excitations [24]. Thus a simple class of trial states is analyzed, namely:

$$|\phi\rangle = \left(a + \sum_{k\alpha} b_{k\alpha} a_{\alpha_1}^\dagger a_{k\alpha} \right) |\psi\rangle \quad (19)$$

with the variational parameters $b_{k\alpha}$ determined so that $\bar{E} \equiv \langle \phi | H(0) | \phi \rangle$ attains its minimum. As a result a simple form for $|\phi\rangle$ is obtained:

$$|\phi\rangle = \frac{1}{\sqrt{n_h d}} \sum_{\alpha} a_{\alpha_1}^\dagger a_{F\alpha} |\psi\rangle \quad (20)$$

where the states $|F\alpha\rangle$ from which the screening electron are removed belong to the Fermi surface, as one would intuitively expect because this yields the lowest possible energy for the screening electron.

With the form of Eq. (20) used in the second term of Eq. (15) the relaxed Auger current due to the decay from the totally relaxed ground-state $|\phi\rangle$ is proportional to a three-body Green density of states:

$$D_{\phi\phi}(\omega) \sim \sum_{\alpha_1, \beta_1} \sum_{\alpha'_1, \beta'_1} M_{ck\alpha_1\beta_1}^* M_{ck\alpha_1\beta_1} D(\alpha_1\beta_1\gamma_1\gamma'_1\beta'_1\alpha'_1; \omega) \quad (21)$$

with:

$$D(\alpha_1\beta_1\gamma_1\gamma'_1\beta'_1\alpha'_1; \omega) = -\frac{1}{\pi} \Im [\text{FT}(\theta(t) G(\alpha_1\beta_1\gamma_1\gamma'_1\beta'_1\alpha'_1; t))] \quad (22)$$

$$G(\alpha_1\beta_1\gamma_1\gamma'_1\beta'_1\alpha'_1; t) = \langle \psi | \mathbb{T} \{ a_{\alpha_1}^\dagger(t) a_{\beta_1}^\dagger(t) a_{\gamma_1}(t) a_{\gamma'_1}^\dagger a_{\beta'_1} a_{\alpha'_1} \} | \psi \rangle \quad (23)$$

So we obtain that the Auger-holes/screening-electron dynamics is described by G_ω ; unfortunately we have no recipes like BLA for the three-body Green's function and the problem of the solution of the Dyson equation for G_ω is much harder than for $G_\omega^{(2)}$. In the next section we will propose a simple recipe for the calculation of G_ω based on some physical approximations.

4. An extended bare ladder approximation

The Green's function (23) yields the expansion:

$$G(\alpha_1\beta_1\gamma_1\gamma'_1\beta'_1\alpha'_1; t) = \sum_n (-1)^n (-i)^{3n+3} \int_{-\infty}^{\infty} dt_1 \dots \int_{-\infty}^{\infty} dt_n \langle \mathbb{T} \{ a_{\alpha_1}^\dagger(t) a_{\beta_1}^\dagger(t) a_{\gamma_1}(t) H_U(t_1) \dots H_U(t_n) a_{\gamma'_1}^\dagger a_{\beta'_1} a_{\alpha'_1} \} \rangle_c \quad (24)$$

This describes the propagation of two-holes and one electron in the final state, or, if the electron and one hole annihilate, a one-body propagation results.

In proposing an approximation to Eq. (24), we may proceed by analogy with $G_\omega^{(2)}$ using separately

the BLA to each two-body interaction [17] (see Fig. 1). Together with the all possible two-body interactions we get a single particle diagram corresponding to the creation of one of the two Auger holes in the screening cloud (the so-called one-body channel for the Auger decay).

However, this approximate solution of the perturbation series does not treat the two Auger holes and screening electron on equal footing and the resulting density of states is not positive defined.

To avoid this problem recently [18] we have proposed for G_ω an extended bare ladder approximation in which all the possible two-body bare interactions are allowed, as shown by the second order diagram of Fig. 2. However, the series cannot be summed easily like in Eq. (12), because with three bodies involved we meet an extra difficulty. For instance, let $H_U(t_i)$ produce an interaction between the two holes in a given term of the expansion; then, the electron line overtakes time t_i ; therefore the diagram does *not* yield a convolution of a function of $t - t_i$ times a function of t_i . This undesirable feature can be removed by using the identities:

$$S_0^h(\alpha_1, \beta_1; t) = i \sum_\gamma S_0^h(\alpha_1, \gamma; t - t') S_0^h(\gamma, \beta_1; t') \quad (25)$$

and

$$S_0^e(\alpha_1, \beta_1; t) = i \sum_\gamma S_0^e(\alpha_1, \gamma; t - t') S_0^e(\gamma, \beta_1; t') \quad (25')$$

where the summations run over all the complete set of spin-orbitals. We note that in the limit $t = t' \rightarrow 0^+$, we get the correct normalization only thanks to the completeness of the γ set.

To see the use of Eqs. (25), consider for instance the application to one of the second-order contributions to Eq. (24). Using the standard diagrammatic rules, we get the l.h.s. of the uppermost equation in Fig. 2, while Eqs. (25), that we represent pictorially as the r.h.s. of the uppermost equation in Fig. 2, permits to write the diagram in a form of a product (in time space) of simple diagrams. In this way, introducing a fictitious \times interaction vertex, along with the true interaction vertex (dot), the diagram is cast in the convolution form. This useful property extends to all the diagrams of the bare-ladder approximation.

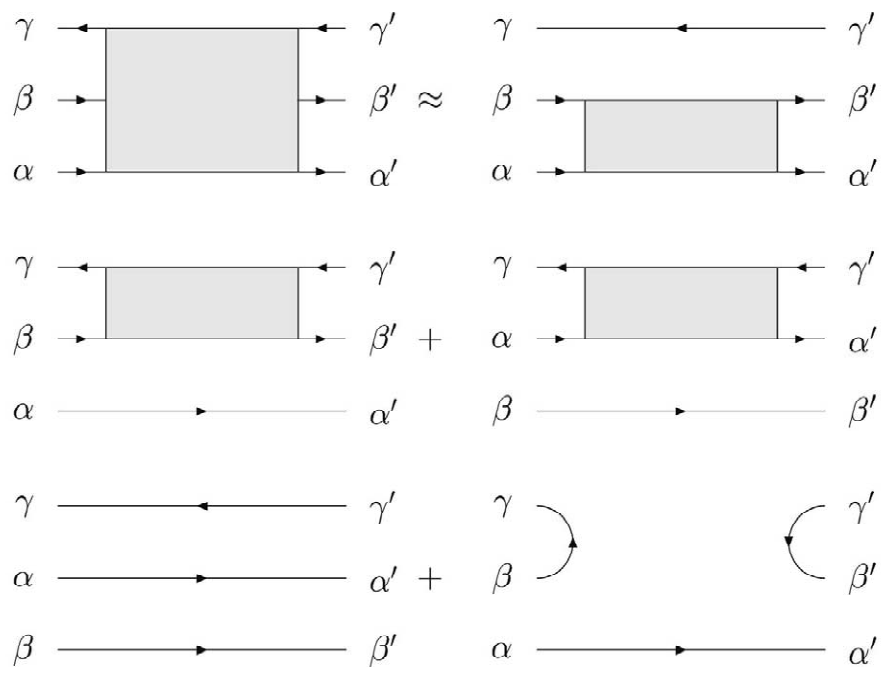
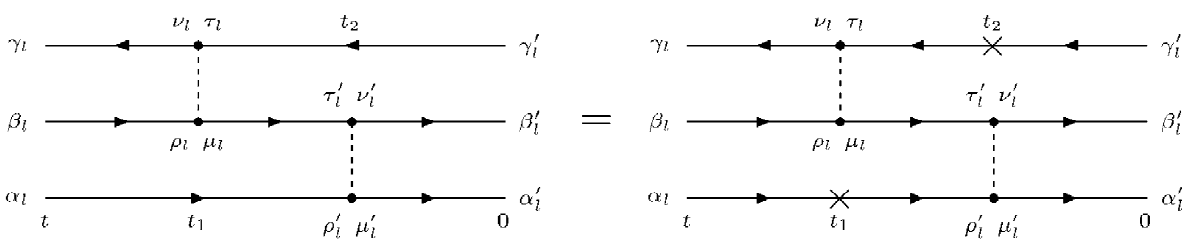


Fig. 1. To a first approximation to Eq. (24) each two-body interaction is solved separately using BLA (represented by the box in all the diagrams on the l.h.s.). The first three diagrams of the l.h.s. represent the hole–hole and the two possible hole–electron series of scattering process; the fourth diagram is a non interacting term necessary to avoid double counting while the last diagram describes the dynamics of the single Auger hole (see text).



where

$$\alpha_l \xrightarrow[t]{t_1} \rho'_l = i \sum_{\alpha} S_0^h(\alpha_l, \alpha; t - t_1) S_0^h(\alpha, \rho'_l; t_1 - t_2)$$

$$\tau_l \xleftarrow[t_1]{t_2} \gamma'_l = i \sum_{\gamma} S_0^e(\tau_l, \gamma; t_1 - t_2) S_0^e(\gamma, \gamma'_l; t_2)$$

Fig. 2. Second order contribution to the three-body Green's function. Using Eqs. (25) we cast it in the form of a product of three 'blocks'. These are easily dealt with by a Fourier transform.

4.1. Core-approximation

Using Eqs. (25) we got a great simplification for the second order diagram of Fig. 2. However, the infinite summations (one for each \times interaction) are a high price to pay for that. They arise because Eqs. (25) imply a summation over the complete set of γ . On the other hand, since we use a *local* H_U , the dot interaction involves only *local* matrix elements between spin-orbitals; so, we are only interested in the *local* elements $S^{\text{h,e}}(\alpha_1, \beta_1; t)$. Physically, we may expect that only the sites which are closest to the Auger site give an important contribution to the summations, and we can actually work with a sum over γ drastically limited to the local states γ_1 . We have observed above that summing over the complete γ set is necessary to get the correct zero-time limit. To preserve normalization using only the local states γ_1 as intermediate states in Eqs. (25) we introduce a set of functions $R^\pm(\alpha_1, \beta_1; t)$ which approximately factor the propagator in analogy with Eqs. (25) according to the ansatz:

$$(-i) \langle a_{\alpha_1}^\dagger(t) a_{\beta_1} \rangle \approx \sum_{\gamma} {}_1R^+(\alpha_1, \gamma_1; t - t') \langle a_{\gamma_1}^\dagger(t') a_{\beta_1} \rangle \quad (26)$$

and

$$(-i) \langle a_{\alpha_1}(t) a_{\beta_1}^\dagger \rangle \approx \sum_{\gamma} R^-(\alpha_1, \gamma_1; t - t') \langle a_{\gamma_1}(t') a_{\beta_1}^\dagger \rangle \quad (26')$$

where t' is any time intermediate between 0 and t ; the $R^{(\pm)}$ functions are computed for any t by solving the system for $t' \rightarrow 0$.

For an isolated core state Green's function we have that:

$$g_c(t) = -ie^{-iEt} \Rightarrow g_c(t) = ig_c(t - t') g_c(t') \quad \forall t' \quad (27)$$

therefore we call the set of Eqs. (26) core approximation (CA).

The ansatz is also correct in the strong coupling case, when localized two-hole resonances develop. This is appealing, since the strong coupling case is the hard one, while at weak coupling practically every reasonable approach yields similar results.

Thus, we regard the ansatz (26) as a physically motivated approximation, which must be tested against exact results for its validation.

4.2. Summing the three-body ladder

Working out the core approximation (CA) like in the second-order case showed in Fig. 2 one can compute all kinds of ladder diagrams, to all orders. The partial sum of the series (24) that one obtains in this way will be referred to as core-ladder-approximation (CLA). From now on only *local* indices appear so we shall dispense ourselves from showing this explicitly. At order n of the perturbation series for G_ω we get the six contributions represented in Fig. 3; Fourier transforming and summing all orders we obtain a linear system of equations for the CLA form $G^{\text{CLA}}(\alpha\beta\gamma, \gamma'\beta'\alpha'; \omega)$ of the three-body Green's function, namely:

$$G^{\text{CLA}}(\alpha\beta\gamma, \gamma'\beta'\alpha'; \omega) = B_0(\alpha\beta\gamma, \gamma'\beta'\alpha'; \omega) - \sum_{\xi} \left\{ \sum_{\mu < \nu} \left[\sum_{\rho < \tau} U_{\mu\nu\rho\tau} B_0(\alpha\beta\gamma, \xi\tau\rho; \omega) \right] \times G^{\text{CLA}}(\mu\nu\xi, \gamma'\beta'\alpha'; \omega) - \sum_{\mu < \nu, \rho < \tau} U_{\mu\nu\rho\tau} B_0(\alpha\beta\gamma, \nu\xi\rho; \omega) \times G^{\text{CLA}}(\mu\xi\tau, \gamma'\beta'\alpha'; \omega) + B_0(\alpha\beta\gamma, \mu\tau\xi; \omega) G^{\text{CLA}}(\xi\nu\rho, \gamma'\beta'\alpha'; \omega) \right\} \quad (28)$$

where the B_0 functions are:

$$\begin{aligned} B_0(\alpha\beta\gamma, \gamma'\beta'\alpha'; \omega) &= G_0(\alpha\beta\gamma, \gamma'\beta'\alpha'; \omega) - G_0(\beta\alpha\gamma, \gamma'\beta'\alpha'; \omega) \\ B_0(\alpha\beta\gamma, \xi\tau\rho; \omega) &= G_0(\alpha\beta\gamma, \xi\tau\rho; \omega) - G_0(\alpha\beta\gamma, \xi\rho\tau; \omega) \\ B_0(\alpha\beta\gamma, \nu\xi\rho; \omega) &= G_0(\alpha\beta\gamma, \nu\xi\rho; \omega) - G_0(\alpha\beta\gamma, \nu\rho\xi; \omega) \\ B_0(\alpha\beta\gamma, \mu\tau\xi; \omega) &= G_0(\alpha\beta\gamma, \mu\tau\xi; \omega) - G_0(\alpha\beta\gamma, \mu\xi\tau; \omega) \end{aligned} \quad (29)$$

As a shorthand notation, we underline the electron indices that correspond to a R^\pm factor; for example:

$$G_0(\alpha\beta\underline{\gamma}, \underline{\xi}\tau\rho; t - t_1) = R^-(\gamma, \xi; t - t_1) S_0^{\text{h}}(\beta, \tau; t - t_1) S_0^{\text{h}}(\alpha, \rho; t - t_1) \quad (30)$$

this is similar to a non-interacting three-body propagator, except that the S^{e} has been replaced by a R^- .

The second, third and fourth lines of (28) come from the (a,b), (c,d) and (e,f) diagrams of Fig. 3, respectively; while the first two contributions come from the hole-hole interaction the others come from

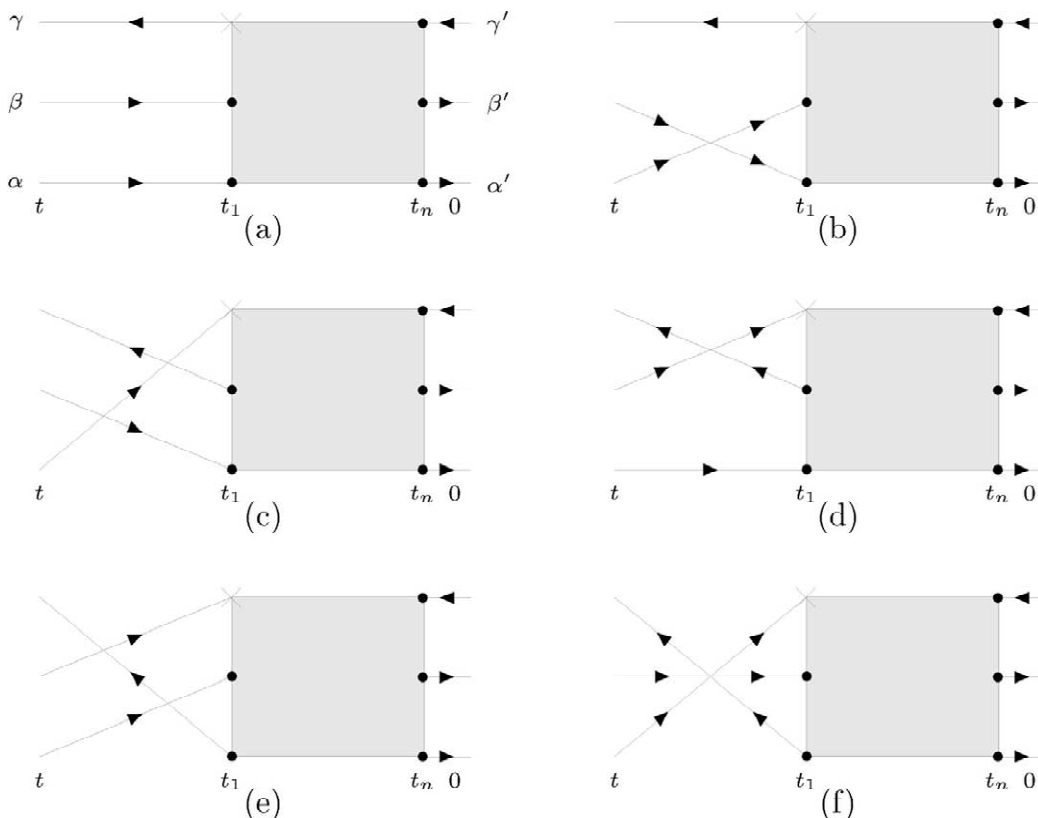


Fig. 3. Diagrammatic representation of the contributions of order n to the CLA (Eq. (28)). The fictitious \times interaction vertex represents a R^{\pm} function.

electron–hole interactions and convey information on the screening effects due to the electronic cloud which forms as a response to the deep electron ionization.

4.3. Single-particle contribution

At the same level of approximation we must consider the case when one (or both) the holes produced by the Auger transitions has the same spin as the screening electron. Consider the spin–diagonal components $G(\alpha\beta\gamma,\gamma'\beta'\alpha';t)$, (with $\sigma_{\alpha'} = \sigma_{\alpha}$ and so on); when the hole β has the same z spin component as the electron, then, contracting $a_{\beta}^{\dagger}(t)$ with $a_{\gamma}(t)$ and $a_{\beta'}$ with $a_{\gamma'}$, in (23) one obtains the extra contribution:

$$G^{\text{sp}}(\alpha\beta\gamma,\gamma'\beta'\alpha';t) = (-1)\langle a_{\beta}^{\dagger}a_{\gamma} \rangle \langle a_{\gamma'}^{\dagger}a_{\beta'} \rangle S(\alpha,\alpha';t) \tag{31}$$

where $S(\alpha,\alpha';t)$ stands for the time-ordered dressed one-body Green’s function that can be expanded with:

$$S(\alpha,\alpha';t) = \sum_n (-i)^n \int_{-\infty}^{\infty} dt_1 \dots \int_{-\infty}^{\infty} \times dt_n \langle T \{ a_{\alpha}^{\dagger}(t) H_u(t_1) \dots H_v(t_n) a_{\alpha'} \} \rangle_c \tag{32}$$

and summed with the Dyson’s equation [27] in terms of proper self-energy diagrams.

Using the general rules of perturbation theory [27] it is possible to show that the self-energy operator is proportional to a three-body Green’s function; namely:

$$\begin{aligned}
S(\alpha, \alpha'; \omega) = & S_0(\alpha, \alpha'; \omega) - \sum_{\mu' < \nu', \rho' < \tau'} \sum_{\mu < \nu, \rho < \tau} U_{\mu\nu\rho\tau} U_{\mu'\nu'\rho'\tau'} \\
& \times \{ [S_0(\alpha, \rho; \omega) G(\mu\nu\tau, \nu'\tau'\rho'; \omega) \\
& - S_0(\alpha, \tau; \omega) G(\mu\nu\rho, \nu'\tau'\rho'; \omega)] S(\mu', \alpha'; \omega) \\
& + [S_0(\alpha, \tau; \omega) G(\mu\nu\rho, \mu'\tau'\rho'; \omega) \\
& - S_0(\alpha, \rho; \omega) G(\mu\nu\tau, \mu'\tau'\rho'; \omega)] S(\nu', \alpha'; \omega) \} \quad (33)
\end{aligned}$$

so we get a conserving approximation for the proper self-energy, using the CLA for the three-body Green's functions of Eq. (33).

By solving Dyson's Eq. (33) one can model XPS spectra from valence bands with low band filling; this is another field of application of our approach.

The deep hole attracts a screening electron that can be directly involved in the Auger decay; this is the physical origin of the contribution (31) to the three-body Green's function. Locally, such processes leave the system with one hole in the final state. The presence of an one-body contribution in the Auger spectra from transition metals like Ti or Sc has been pointed out already [16,17]. Besides the three-body (28) and one-body (31) diagrams, there are mixed contributions as well. Physically they represent interference terms in which the system evolves from one-hole states to two-holes-one-electron states and back. However such terms can be neglected [18]; the final result is:

$$\begin{aligned}
G(\alpha\beta\gamma, \gamma' \beta' \alpha'; \omega) = & G^{\text{CLA}}(\alpha\beta\gamma, \gamma' \beta' \alpha'; \omega) \\
& + G^{\text{SP}}(\alpha\beta\gamma, \gamma' \beta' \alpha'; \omega). \quad (34)
\end{aligned}$$

4.4. A model cluster calculations

CLA results have been tested against those of a model system that can be diagonalised exactly [18].

The model was a five atom cluster, with two levels for each atom; the one-body basis elements are $|s_i\sigma\rangle$ with $s = 1, \dots, 5$ the site index, $i = 1, 2$ the level index and $\sigma = \uparrow, \downarrow$ for the spin direction; the one-body energies are denoted by ϵ_{s_j} . The atoms 1...4 occupy the vertices of a square, and the Auger atom is at site 5 above the center. The system's dynamics is given by an Hubbard-like Hamiltonian composed of a one-body Hamiltonian H_0 , of the same level of sophistication as a tight-binding model of a solid, with a nearest neighbor hopping term:

$$H_0 = \sum_{s_i\sigma} n_{s_i\sigma} \epsilon_{s_i} + \sum_{ij\sigma} \sum_{\langle ss' \rangle} T_{ij}^{ss'} a_{s_i\sigma}^\dagger a_{s'j\sigma} \quad (35)$$

with real $T_{ij}^{ss'}$. Next the interactions are described by an Hubbard term:

$$H_{\text{Hub}} = U \left[\sum_{sij} n_{s_i\uparrow} n_{s_j\downarrow} + \sum_{s\sigma} n_{s1\sigma} n_{s2\sigma} \right] \quad (36)$$

subtracted of a Hartree–Fock mean field average of the interaction so that the total hamiltonian reads:

$$H = H_0 + H_{\text{Hub}} - V_{\text{H-F}} \quad (37)$$

and in this way, the Hartree–Fock contribution to the self-energy would be automatically embodied in the bare propagators.

By considering various possible electron populations $N \leq 20$ in the cluster, the mean occupation of the Auger site in the non-interacting ground state:

$$\langle n \rangle = \frac{1}{4} \sum_{\sigma} \langle n_{51\sigma} + n_{52\sigma} \rangle \quad (38)$$

was varied. The test becomes more severe when $\langle n \rangle$ is reduced towards half filling and U/W is increased. Many different densities of states are obtained from the matrix elements of $G(\omega)$; in the context of our theory, the density:

$$\begin{aligned}
D_{1h}(\omega) \equiv & \langle \psi | a_{51\uparrow}^\dagger a_{52\downarrow}^\dagger a_{51\uparrow} \delta(\omega + H \\
& - E) a_{51\uparrow}^\dagger a_{52\downarrow} a_{51\uparrow} | \psi \rangle \quad (39)
\end{aligned}$$

is of special interest because in the diagrammatic series the annihilation of the spin-up electron by the hole of the same spin is particularly strong so we may expect that the one-body term is important. By contrast, in the density:

$$\begin{aligned}
D_{2h1e}(\omega) \equiv & \langle \psi | a_{51\uparrow}^\dagger a_{51\downarrow}^\dagger a_{52\uparrow} \delta(\omega + H \\
& - E) a_{52\uparrow}^\dagger a_{51\downarrow} a_{51\uparrow} | \psi \rangle \quad (40)
\end{aligned}$$

the same contribution should be smaller and possibly absent. Although the analytic development can be somewhat boring, the maximum size of the matrices involved is just 8.

Fig. 4 shows D_{1h} for $U/W=1$ with a population $\langle n \rangle = 0.86$ and $\langle n \rangle = 0.72$ on the Auger site. The density is dominated by a single peak at binding

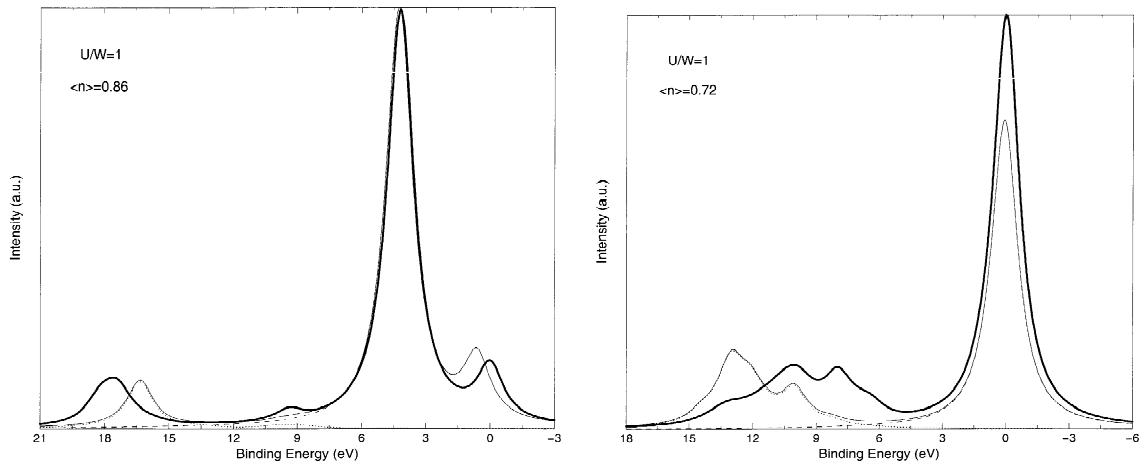


Fig. 4. Binding energy dependence of D_{1h} for $U/W=1$ and $\langle n \rangle = 0.86$ (left frame) and $\langle n \rangle = 0.72$ (right frame). Heavy line: exact result; light: CLA; dashed: 1-body contribution to the CLA result; dotted: 3-body contribution to the CLA result. The line shapes have been convolved with a Lorentzian (FWHM=0.75 eV).

energy ≈ 4 eV, but also shows a pair of wings. The value of U is well outside the scope of weak coupling approaches but for $\langle n \rangle = 0.72$ the CLA reproduces the exact results rather well. A shift (≈ 5 eV) and an increase of the structure at high binding energy is understandable because the filling is high and the screening ineffective. From these first results we see that the performance of the CLA does not break down quickly with increasing U as weak-coupling approaches tend to do, but remains fairly

stable. The CLA also explains the increase of the relative weight of the 3-body contribution with reducing band filling.

As one could expect, $D_{2h1e}(\omega)$ has much more weight at high binding energies than $D_{1h}(\omega)$, as one can see in Fig. 5; in both frames $\langle n \rangle = 0.72$ but the interaction increase from $U/W=0.25$ (left frame) to $U/W=1$ (right frame).

For $U/W=0.25$ the agreement is fairly good. For $U/W=1$ the exact line shape shows three partially

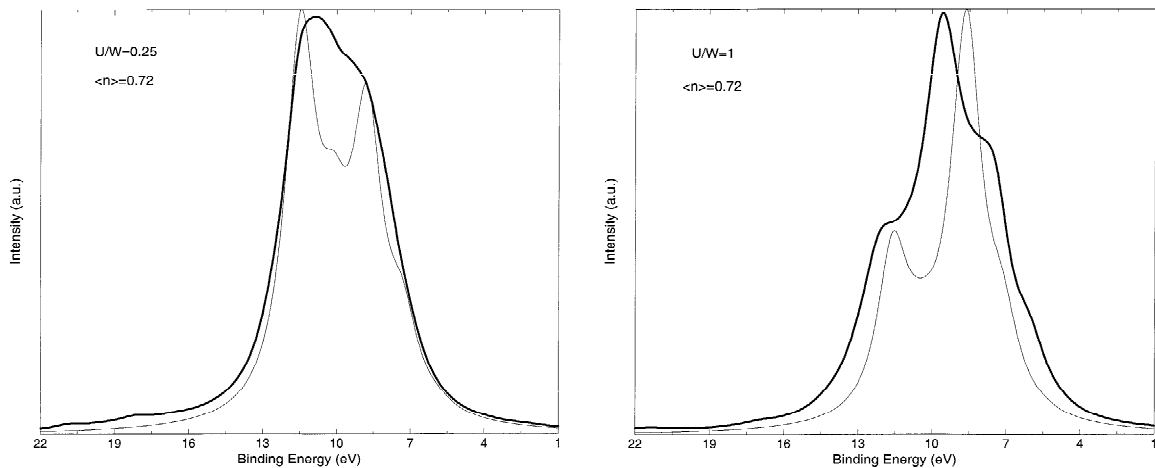


Fig. 5. Binding energy dependence of D_{2h1e} for $\langle n \rangle = 0.72$ and $U/W=0.25$ (left frame) and $U/W=1$ (right frame). Heavy line: exact result; light: CLA; dotted: 3-body contribution to the CLA result. The line shapes have been convolved with a Lorentzian (FWHM=0.75 eV). Note that for $\langle n \rangle = 0.72$ no single-particle contribution exists because $\langle \psi | a_{51\uparrow}^\dagger a_{52\uparrow} | \psi \rangle = 0$.

resolved broad peaks covering a range of ≈ 10 eV in binding energy. The CLA misses the main peak position by ≈ 1 eV and undervaluates the low binding energy shoulder; however, we can still claim at least a qualitative agreement with the results of the exact calculation in such severe conditions.

In all cases we verify that the Herglotz property is fully preserved; this is a most valuable feature which is not easily obtained for approximate three-body propagators. For instance, the approach of Ref. [17] fails in this respect at strong coupling.

Comparing the two frames of Fig. 5 we observe the apparent negative- U behavior: increasing the interaction U , the main peak shifts towards lower binding energies; this is a consequence of the interaction of the screening electron with the two Auger holes. We remark that a high enough n_h is necessary to build up a localized screening cloud. This is why the negative- U behavior is observed in the early transition metals, but not in the late ones.

5. Conclusions

We have proposed a model where the ' $U < 0$ ' behavior of the Auger and APECS line shapes of early transition metals is described by a three-body Green's function dynamics. The solution of the two-holes-one-electron perturbation series is a formidable problem that we solve proposing the core-ladder-approximation: a new approach based on physical approximations and results valid for the two-holes case. The CLA is the first step of a procedure which eventually leads to the exact summation of the 3-body ladder series. Like perturbation theory and other approaches to the many-body problem, it allows systematic improvements at the cost of more computation.

Physically CLA is well motivated and well balanced, and cluster calculations provide evidence that it correctly describes the effect of the screening electron over the two final-state holes. The property of the CLA of remaining qualitatively correct even at rather strong coupling, conserving the Herglotz property, is an important feature. The success of CLA depends on the fact that the core approximation becomes accurate at strong coupling, and permits to

treat the screening electron and the Auger holes on equal footing.

Further applications of CLA are possible: first the Coster–Kronig $CC'V$ decay followed by Auger $C'VV$ transition that leaves three holes in the valence bands; CLA provides a method to calculate the final state dynamics. Moreover the sum of the perturbation series of the three-body Green's function can be used to construct a self-energy operator that can work outside the low-density regime of the usual T-matrix approach.

Acknowledgements

This work has been supported by the Istituto Nazionale di Fisica della Materia. One of us (AM) has been supported by the INFN scholarship 'Analisi teorica della Tecnica A.P.E.C.S.', prot. 1350.

References

- [1] O. Gunnarsson, K. Schönhammer, Phys. Rev. B 22 (1980) 3710.
- [2] P. Weightman, Rep. Prog. Phys. 45 (1982) 753; J.C. Riviere, Atomic Energy Research Report AERE-R10384, 1982.
- [3] M. Cini, Solid State Commun. 20 (1976) 605.
- [4] M. Cini, Solid State Commun. 24 (1977) 681.
- [5] G.A. Sawatzky, Phys. Rev. Lett. 39 (1977) 504.
- [6] C. Verdozzi, M. Cini, J.F. McGilp, G. Mondio, D. Norman, J.A. Evans, A.D. Laine, P.S. Fowles, L. Duò, P. Weightman, Phys. Rev. B 43 (1991) 9550.
- [7] R.J. Cole, C. Verdozzi, M. Cini, P. Weightman, Phys. Rev. B 49 (1994) 13329.
- [8] C. Verdozzi, M. Cini, J.A. Evans, R.J. Cole, A.D. Laine, P.S. Fowles, L. Duò, P. Weightman, Europhys. Lett. 16 (8) (1991) 743; M. Cini, C. Verdozzi, Physica Scripta T 41 (1992) 67; C. Verdozzi, M. Cini, Phys. Rev. B 51 (1995) 7412.
- [9] M. Cini, Surf. Sci. 87 (1979) 483.
- [10] V. Galitzkii, Soviet Phys. JEPT 7 (1958) 104.
- [11] M. Cini, C. Verdozzi, J. Phys. C 1 (1989) 7457.
- [12] M. Cini, M. De Crescenzi, F. Patella, N. Motta, M. Sastry, F. Rochet, R. Pasquali, A. Balzarotti, C. Verdozzi, Phys. Rev. B 41 (1990) 5685.
- [13] J.E. Houston, J.W. Rogers, R.R. Rye, F.L. Hutson, D. Ramaker, Phys. Rev. B 34 (1986) 1215; M. Cini, A. D'Andrea, in: K. Wandelt, G. Mondio, G. Cubiotti (Eds.), Auger Spectroscopy and Electronic Struc-

- ture, Springer Series in Surface Science, Vol. 18, Springer, Heidelberg, 1989.
- [14] P. Hedegård, F.U. Hillebrecht, *Phys. Rev. B* 34 (1986) 3045.
- [15] D.K.G. de Boer, C. Haas, G.A. Sawatzky, *J. Phys. F* 14 (1984) 2769.
- [16] D.D. Sarma, S.R. Barman, S. Nimkar, H.R. Krishnamurthy, *Phys. Scripta* 41 (1992) 184.
- [17] M. Cini, V. Drchal, *J. Phys. C* 6 (1994) 8549;
M. Cini, V. Drchal, *J. Electron Spectrosc. Relat. Phenom.* 72 (1995) 151.
- [18] A. Marini, M. Cini, *Phys. Rev. B* 60 (1999) 11391.
- [19] H.W. Haak, G.A. Sawatzky, T.D. Thomas, *Phys. Rev. Lett.* 41 (1978) 1825.
- [20] H.W. Haak, G.A. Sawatzky, L. Ungier, J.K. Gimzewsky, T.D. Thomas, *Rev. Sci. Instrum.* 55 (1984) 696.
- [21] G.A. Sawatzky, *Auger Photoelectron Coincidence Spectroscopy*, Treatise On Material Science and Technology, Vol. 30, Academic Press, New York, 1990.
- [22] E. Jensen, R.A. Bartynski, S.L. Hulbert, E.D. Johnson, *Rev. Sci. Instrum.* 63 (1992) 3013.
- [23] G.A. Sawatzky, A. Lenseink, *Phys. Rev. B* 21 (1980) 1390.
- [24] O. Gunnarsson, K. Schönhammer, *Phys. Rev. B* 26 (1982) 2765.
- [25] M. Cini, C. Verdozzi, *Solid State Commun.* 57 (1986) 657.
- [26] P.W. Anderson, *Phys. Rev. Lett.* 18 (1967) 1049.
- [27] R.D. Mattuck, *A Guide To Feynman Diagrams in the Many-Body Problem*, McGraw-Hill, New York, 1976, Chapter 10.